Electronic Supplementary Information

for:

Facile high-yield synthesis and purification of lysine modified graphene oxide for enhanced drinking water purification

Sebastiano Mantovani,[a†] Sara Khaliha,[a†] Tainah Dorina Marforio,[b†] Alessandro Kovtun,[a] Laura Favaretto,[a] Francesca Tunioli,[a] Antonio Bianchi,[a] Gaetana Petrone,[c] Andrea Liscio,[c] Vincenzo Palermo,[a,*] Matteo Calvaresi,[b,*] Maria Luisa Navacchia,[a] Manuela Melucci [a,*]

[a.] Consiglio Nazionale delle Ricerche, Institute of Organic Synthesis and Photoreactivity (CNR-ISOF) via Piero Gobetti 101, 40129 Bologna- Italy

[b.] Alma Mater Studiorum - University of Bologna, Department of Chemistry 'G. Ciamician', via Selmi 2, 40129 Bologna-Italy

[c.] Consiglio Nazionale delle Ricerche, Institute for Microelectronics and Microsystems (CNR-IMM), via del fosso del cavaliere 100, 00133 Roma- Italy

Contents:

11. Adsorption isotherms

1. Selected contaminants

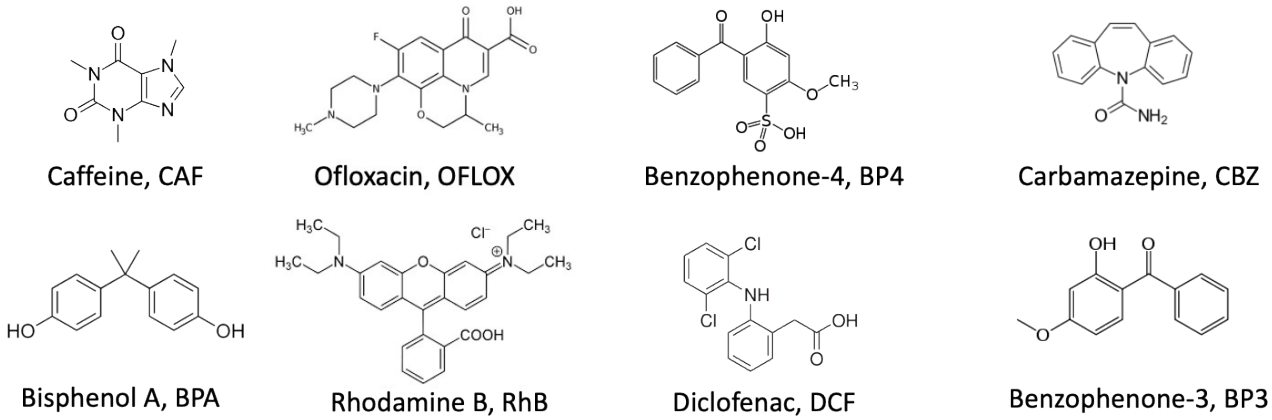

Fig. S1. Molecular structure of selected contaminants.

2. Adsorption capacity of BPA, CBZ, BP4, state of the art

Table S1. Adsorption capacity of BPA from literature.

Adsorbents	**Qm BPA (mg/g)**
Reduced Graphene[1]	181.6
Commercial chitosan[2]	27.02
Commercial activated carbon[3]	307
Multi-walled carbon nanotubes[4]	111.1
Cyclodextrin-carboxymethylcellulose-based hydrogel[5]	38.12
Fe_3O_4@plyaniline core-shell nanomaterials[6]	23.09

Table S2. Adsorption capacity of CBZ from literature.

Adsorbents	Qm CBZ (mg/g)
Polypyrrole–Chitosan–Fe_3O_4[7]	121.95
Expanded graphite[8]	43.54
Fe/Cu Nanoparticles[9]	13.07
Fe_3O_4 NPs[10]	44.75
Fe_3O_4-MAA[10]	77.30
Fe_3O_4-SiO_2[10]	65.05
CuO/Cu_2O/Cu-biochar composite[11]	21.83

Table S3. Adsorption capacity of BP4 from literature.

Adsorbents	Qm BP4 (mg/g)
Tertiary amine-functionalized resins[12]	154
Anion Exchange Resin (AER)[12]	91.57
macroporous resin XAD-4 without charged func-tional groups[12]	2.205
Cation exchange resin CER) carboxyl groups[12]	1.032
Activated Carbon (AC) F400[12]	103.6

3. Materials

Commercially available chemicals were purchased from Sigma Aldrich used without any further purification and Graphene Oxide powder were purchased from Abalonyx (S-126/36).

4. Synthesis of GO-NaOH

20 mL of NaOH aqueous solution (2.5 M) were added to 100 mL of an aqueous suspension of GO (5 mg/mL) obtained sonicating 500 mg of material in 100 mL of MilliQ water for 2 h. The mixture was then stirred at 80 °C for 24 h. After this time the crude was purified by reiterated centrifugation until a neutral pH was measured in the washing water. After purification and freeze drying 490 mg of GO-NaOH were obtained. In total 1.2L of water were used for the purification.

5. X-Ray Photoelectron spectroscopy (XPS)

High-resolution XPS by using a Phoibos 100 hemispherical energy analyser (Specs GmbH, Berlin, Germany), using Mg Kα radiation (ħω = 1,253.6 eV; X-Ray power = 125W) in constant analyser energy (CAE) mode, with analyser pass energies of 10 eV. Base pressure in the analysis chamber during analysis was $4.2x10^{-8}$ mbar. Spectra were fitted by using CasaXPS (www.casaxps.com) after Shirley background subtraction and all spectra were calibrated to the C_{1s} binding energy (285.0 eV). XPS samples were prepared by preparing a tablet from the dry powder of each material and fixing it on the sample holder by conductive carbon tape. The pristine GO presents C 1s, O 1s, N 1s, Cl 2p and S 2p signals. The control sample GO-NaOH is slightly reduced, a small amount of Na was present (Na KLL signal) and the Ca 2p signal was due to tap water residuals after washing. GO-Lys present a significantly higher amount of N respect to the pristine GO, the overall oxidation (O 1s / C 1s) was lower than GO due to the presence of aliphatic chains of Lysine.

Table S4. Atomic composition of GO, GO-NaOH and GO-Lys.

Material	Atomic composition (%)						
	C	**O**	**N**	**Na**	**Cl**	**S**	**Ca**
GO	70.4	27	0.7	-	0.8	1	-
GO-NaOH	70.4	25.6	0.2	0.2	0.3	-	3.3
GO-Lys	81.5	13.9	3.1	1.2	0.2	-	-

6. Attenuated total reflection Infrared Spectroscopy (ATR-FTIR)

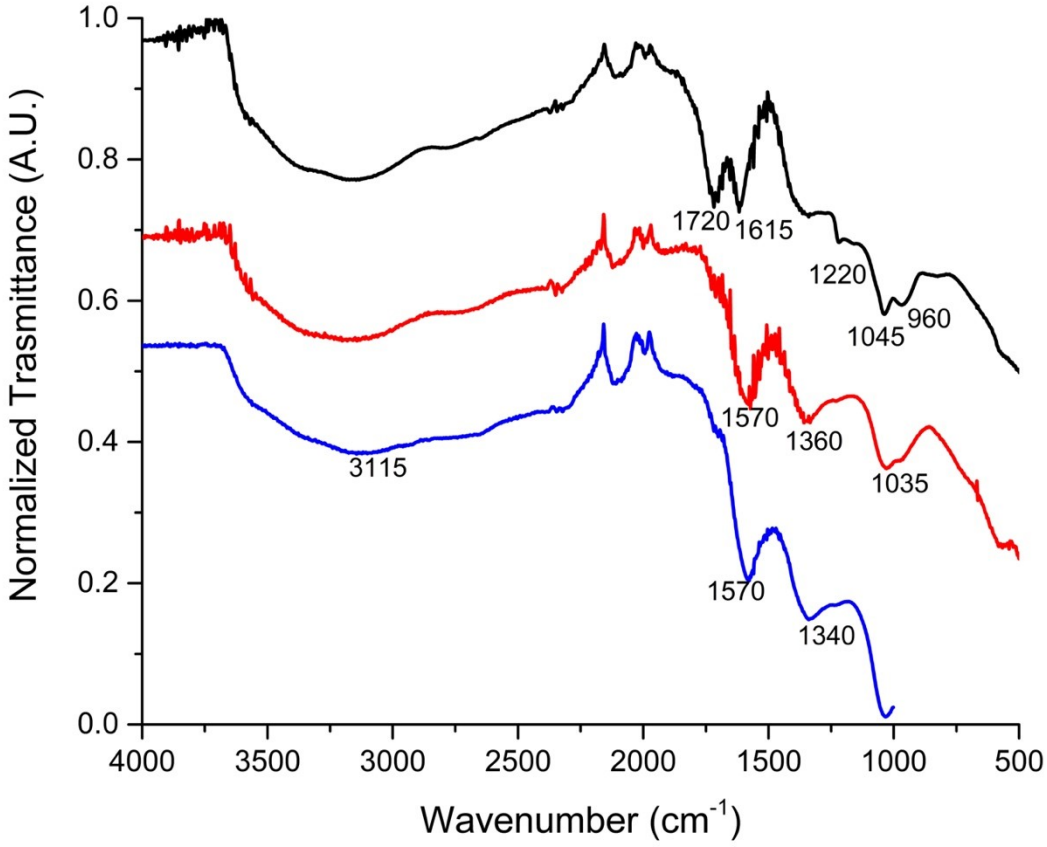

Fig. S2. ATR-FTIR spectra of GO (black line), GO-NaOH (red line) and GO-Lys (blue line).

7. Thermogravimetric analysis (TGA)

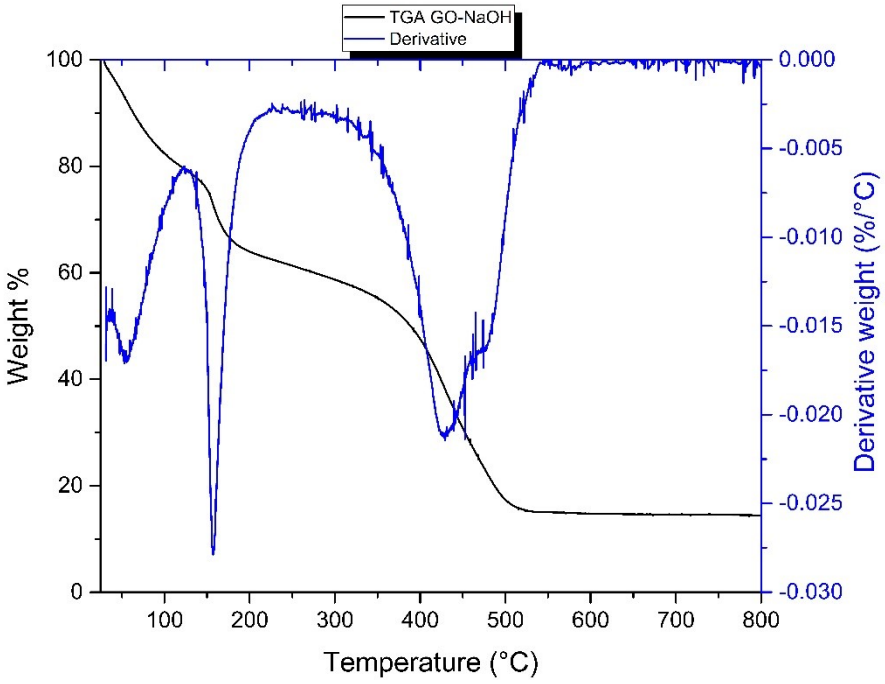

Fig. S3. TGA of GO-NaOH (10°C/min in air).

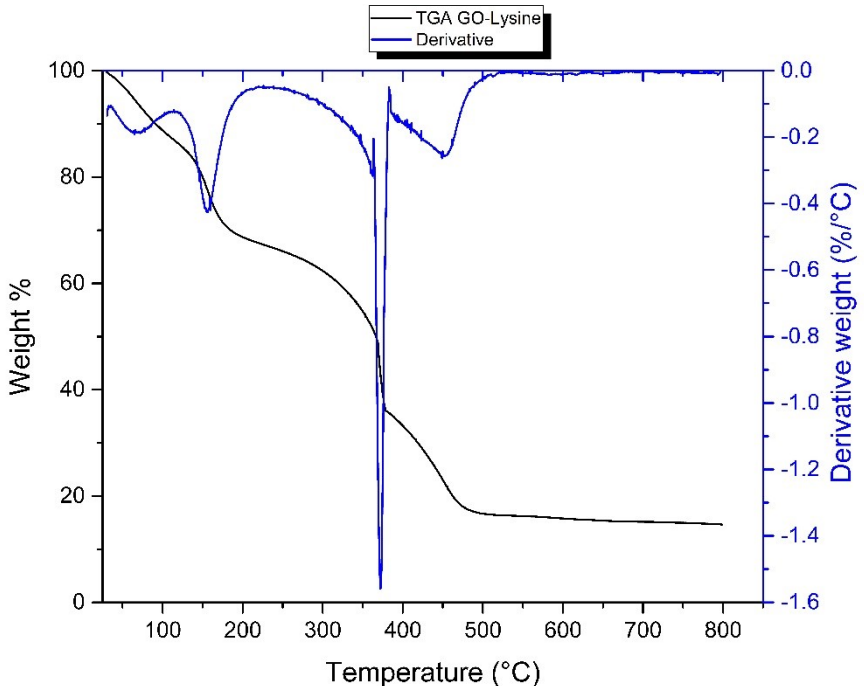

Fig. S4. TGA of GO-Lys (10°C/min in air).

8. Morphological analysis

Lateral size distribution of GO and GO-Lys nanosheets used for the adsorption measurements were performed by the statistical analysis of Scanning electron microscopy (SEM) images acquired using a FEI Dual Beam system (FIB-SEM) 235 with a 1 nm electron beam. Due to the purely 2D nature of the nanosheets and their irregular shape we used the area (A) as a standard morphological parameter. The area of each nanosheet were measured objectively, pixel by pixel, using Spip™ software. Then, the lateral size (s) is defined as the root mean square of the area: $s = \sqrt{A}$.

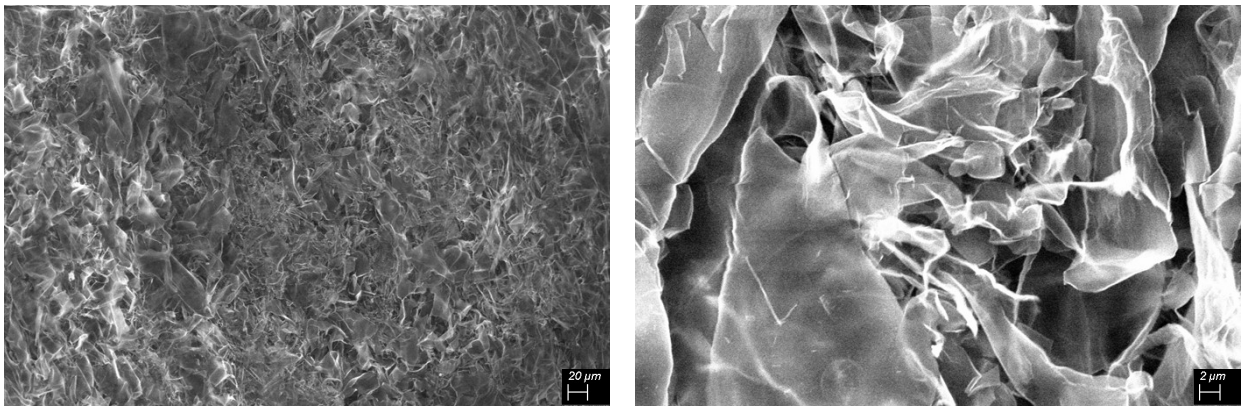

Fig. S5. SEM images of GO-Lys powder after lyophilization. The sample was then sonicated and cast for size analysis.

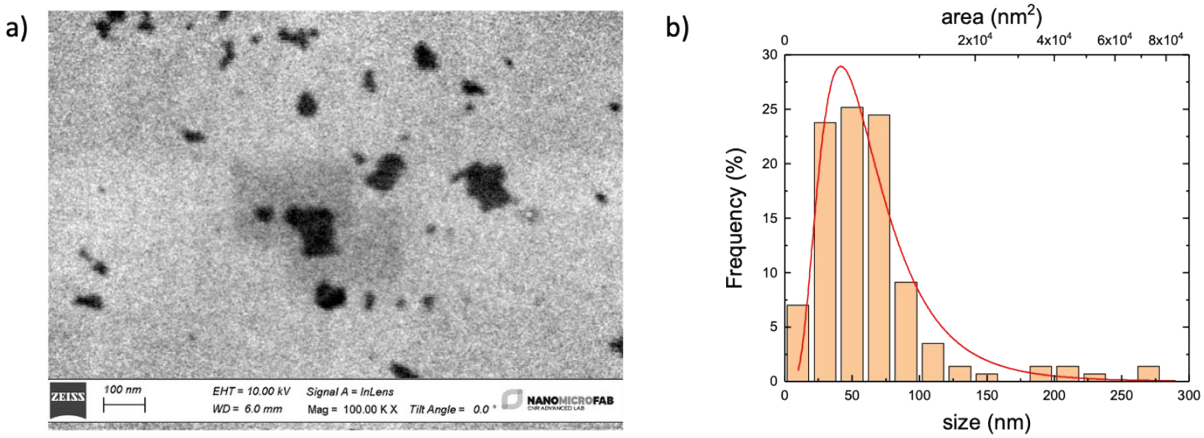

Fig. S6. a) High resolution SEM image GO-Lys nanosheets after 2 hs mild sonication in water dispersion. Total number of nanosheets = 264 and 298, respectively.; b) Lateral size distribution of GO-Lys nanosheets. Log-normal best-fit (red line) for sake of comparison. Total number of nanosheets = 298.

Table S5. Mean area <A> with standard error and corresponding mean lateral size <s>.

	<A> (± standard error) (nm^2)	**<s> (± standard error) (nm)**
GO pristine	6370 (± 870)	63 (± 4)
GO-Lys	6050 (± 940)	63 (± 5)

9. High Performance Liquid Chromatography (HPLC)

ECs analyses were performed by HPLC on a Dyonex Ultimate 3000 system equipped with a diode array detector. 0.5 mL samples were used as sources for the automated injection. LC-MS grade acetonitrile was purchased from Sigma-Aldrich in the highest available purity and used without any further purification. The chromatographic separation was performed on a reverse phase analytical column (Agilent Eclipse XDB-C8 4.6 x 150 mm, 5 μm) at flow rate of 1.0 mL/min, linear gradient TFA 0.05% aqueous solution/acetonitrile from 80:20 to 0:100, detection at λ_{max} of each analyte. In case of the absorption experiments on the selected ECs in mixture the % removal of the analytes was determined by comparison with that of the initial untreated solution. The results are expressed as the mean of two independent experiments ± SD.

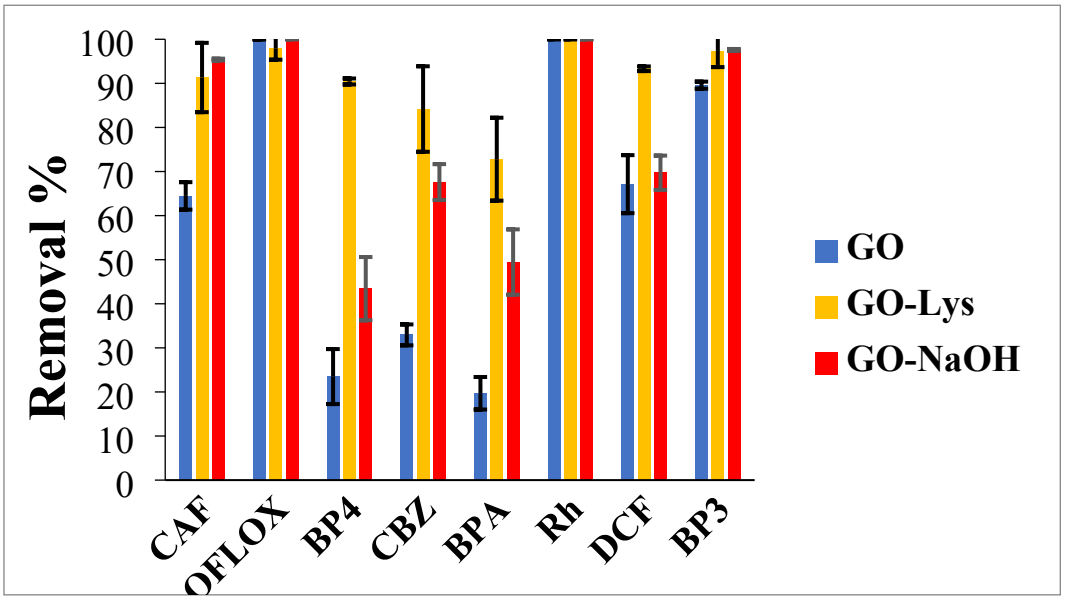

Fig. S7. Removal of ECs mix (5 ppm each, Vtot= 25 ml, 25 mg of sorbent) 1h contact time.

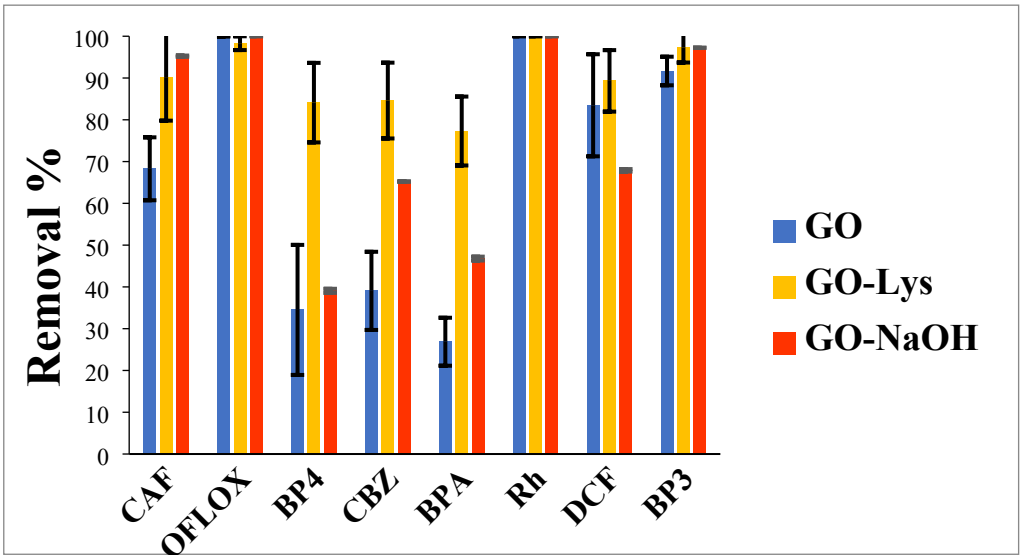

Fig. S8. Removal of ECs mix (5 ppm each, Vtot= 25 ml, 25 mg of sorbent) 4h contact time.

10. Computational details

The gaff force field was used to parameterize CAF, OFLOX, BP4, CBZ, BPA, Rh DCF and BP3 molecules.
Atomic charges were obtained by standard procedures, using QM calculations at the HF/6-31G(d) level of theory, followed by RESP fitting.
The model-systems representing GO and GO-Lys were modelled on a 40 Å x 40 Å graphene sheet created with VMD. The epoxy, hydroxyl, carbonyl, and carboxylic acid groups were randomly positioned on graphene sheet to reproduce the experimental XPS data. The gaff force field was also used to describe GO and GO-Lys. In this case the atomic charges were obtained by AM1 calculations.
An accurate sampling of the interactions was carried out placing the molecules on 16 different positions of the graphene sheet. Each complex was inserted into a box of TIP3P water molecules and counterions were added to neutralize the total charge.
The resulting systems were minimized performing two Molecular Mechanics (MM) minimization steps. In the initial stage, we imposed harmonic constraints (500 kcal mol^{-1} A^{-2}) on the solute (molecule/ graphene complexes) relaxing only the position of waters molecules and ions. During the second minimization step, both the solute and solvent molecules were free to move. Then, the resulting minimized systems were used as starting points for MD simulations. An equilibration step of 10 ns was carried out gradually heating the system from 0 to 298 K, using an Andersen thermostat and periodic boundary conditions (PBC). After the heating step, we carried out production runs of molecular dynamics (MD) simulations of 100 ns.
Molecular Mechanics – Generalized Born Surface Area (MM-GBSA) method, implemented in Amber 16. software package, was applied to compute the binding affinity of molecules to GO and GO-Lys.
For each calculation, 5000 frames were used, extracting the snapshots from the MD trajectories.
The geometric analysis of the MD trajectories was carried out using CPPTRAJ, as implemented in Amber 16.

Table S5. Computed total binding affinity and its contributes (VDW, Electrostatic and E_{SURF}) of the contaminants towards GO. All energies are reported in kcal/mol.

	VDW	**Electrostatic**	**E_{SURF}**	**Total Binding Affinity**
CAF	-28.9	5.7	-0.1	**-22.4**
OFX	-31.1	10.1	-1.2	**-22.2**
BP4	-20.9	10.1	-1.1	**-11.9**
CBZ	-21.8	4.2	-0.7	**-18.4**
BPA	-19.2	4.4	-0.8	**-15.7**
BP3	-24.8	5.8	-0.8	**-19.7**
RhB	-31.6	7.7	-1.6	**-25.6**
DCF	-26.0	6.2	-0.9	**-20.8**

Table S6. Computed total binding affinity and its contributes (VDW, Electrostatic and E_{SURF}) of the contaminants towards GO-Lys. All energies are reported in kcal/mol.

	VDW	**Electrostatic**	**E_{SURF}**	**Total Binding Affinity**
BP4	-32.9	14.4	-2.9	**-21.4**
CBZ	-22.1	4.5	-2.6	**-22.0**
BPA	-21.3	5.6	-2.4	**-18.1**

Table S7. Mean distance of the Lysine side-chain atoms from the basal plane of GO-Lys in the MD trajectories. All values are in Angstrom.

Atom	Distance [Å]
CB	3.9
CG	3.8
CD	3.7
CE	3.7
NZ	3.4

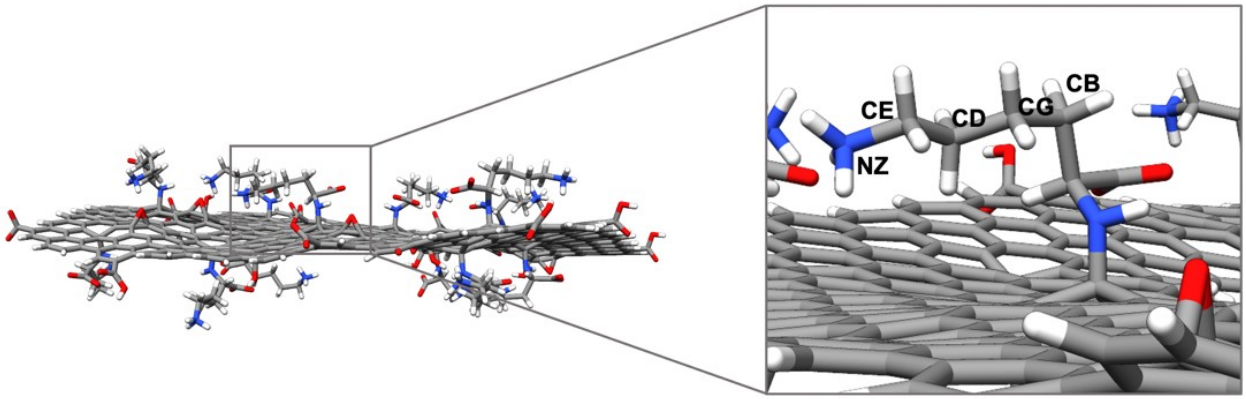

Fig. S9. Lysine side-chain atoms from the basal plane of GO-Lys in the MD trajectories.

11. Adsorption isotherms

Stock solutions of each contaminant were prepared in MilliQ water, according to the maximum solubility of each molecule: BP4 1 mg/mL, BPA 0.3 mg/mL and CBZ 0.1 mg/mL. For each sorbent, two suspensions were prepared, 2 mg/mL and 3 mg/mL in MilliQ water and used after 2 hs of sonication. A different amount of graphene suspension was added to a solution of contaminant (BP4, BPA or CBZ) at different initial concentrations. The solutions (total volume 5 mL) were gently stirred in darkness for 4 hs and then centrifuged at 15,000 rpm for 10 min. The solutions were analyzed by UV-vis spectroscopy or HPLC. Same procedure was performed for each pair sorbent-sorbates, varying the ratio due to the different adsorption capacity. Langmuir and Brunauer–Emmett–Teller (BET) model were used to fit the adsorption data obtained.

Table S8-S10. Experimental parameters of solutions used for isotherms studies.

Table S8.

GO Abalonyx								
SAMPLE	**C_0 BP4 (mg/mL)**	**GO (mg)**	**SAMPLE**	**C_0 BPA (mg/mL)**	**GO (mg)**	**SAMPLE**	**C_0 CBZ (mg/mL)**	**GO (mg)**
1	0.5	7	1	0.24	3	1	0.07	4
2	0.5	5	2	0.24	2	2	0.06	6
3	0.25	5	3	0.15	5	3	0.06	4
4	0.1	10	4	0.015	3	4	0.05	7
5	0.1	5	5	0.09	7	5	0.025	4
6	0.05	10	6	0.09	5	6	0.025	2
7	0.01	10	7	0.09	3	7	0.01	4
			8	0.06	5	8	0.01	2
			9	0.06	3			

Table S9.

GO-NaOH								
SAMPLE	**C_0 BP4 (mg/mL)**	**GO (mg)**	**SAMPLE**	**C_0 BPA (mg/mL)**	**GO (mg)**	**SAMPLE**	**C_0 CBZ (mg/mL)**	**GO (mg)**
1	0.8	5	1	0.24	3	1	0.09	1
2	0.5	5	2	0.15	5	2	0.07	4
3	0.25	3	3	0.15	3	3	0.07	2
4	0.25	5	4	0.09	5	4	0.05	5
5	0.1	3	5	0.09	1	5	0.05	3
6	0.1	4	6	0.06	3	6	0.05	1
7	0.05	2	7	0.06	1	7	0.025	4
8	0.05	3	8	0.024	3	8	0.025	2
9	0.01	1				9	0.01	1
10	0.01	1						

Table S10.

GO-Lys								
SAMPLE	**C_0 BP4 (mg/mL)**	**GO (mg)**	**SAMPLE**	**C_0 BPA (mg/mL)**	**GO (mg)**	**SAMPLE**	**C_0 CBZ (mg/mL)**	**GO (mg)**
1	0.8	3	1	0.3	3	1	0.09	3
2	0.8	1	2	0.27	3	2	0.09	2
3	0.5	5	3	0.25	5	3	0.09	1
4	0.5	3	4	0.25	3	4	0.08	3
5	0.25	5	5	0.15	3	5	0.08	2
6	0.25	3	6	0.125	5	6	0.08	1
7	0.125	5	7	0.125	3	7	0.05	2
8	0.125	3				8	0.025	2

Table S11-S13. Adsorption model and complete fitting for all isotherms.

Table S11. BP4 isotherm

	Langmuir $Q_e = Q_m \cdot \frac{C_e \cdot K_L}{1 + K_L \cdot C_e}$			**BET** $Q_e = \frac{Q_m \cdot C_{BET} \cdot x}{(1-x) \cdot (1 + C_{BET} \cdot x - x)}, \quad x = \frac{C_e}{C_s}$			
	Q_m *[mg/g]*	**K_L** *[mL/mg]*	**R^2**	**Q_m** *[mg/g]*	**C_s** *[mg/mL]*	**C_{BET}**	**R^2**
GO	45 ± 18	4	0.311	11 ± 5	0.6	18	0.772
GO-NaOH	62 ± 12	22	0.989	21 ± 4	1	46	0.884
GO-Lys	292 ± 30	8	0.986	117 ± 23	1	85	0.779

Table S12. BPA isotherm

	Langmuir $Q_e = Q_m \cdot \frac{C_e \cdot K_L}{1 + K_L \cdot C_e}$			**BET** $Q_e = \frac{Q_m \cdot C_{BET} \cdot x}{(1-x) \cdot (1 + C_{BET} \cdot x - x)}, \quad x = \frac{C_e}{C_s}$			
	Q_m *[mg/g]*	**K_L** *[mL/mg]*	**R^2**	**Q_m** *[mg/g]*	**C_s** *[mg/mL]*	**C_{BET}**	**R^2**
GO	33 ± 7	30	0.200	14 ± 5	0.22	70	0.818
GO-NaOH	48 ± 15	19	0.970	16 ± 4	0.3	63	0.897

GO-Lys	295 ± 50	43	0.981	142 ± 35	0.3	70	0.955

Table S13. CBZ isotherm

	Langmuir $Q_e = Q_m \cdot \frac{C_e \cdot K_L}{1 + K_L \cdot C_e}$			**BET** $Q_e = \frac{Q_m \cdot C_{BET} \cdot x}{(1-x) \cdot (1 + C_{BET} \cdot x - x)}$, $x = \frac{C_e}{C_s}$			
	Q_m *[mg/g]*	**K_L** *[mL/mg]*	**R^2**	**Q_m** *[mg/g]*	**C_s** *[mg/mL]*	**C_{BET}**	**R^2**
GO	7 ± 2	86	0.939	2 ± 0.4	0.08	52	0.908
GO-NaOH	80 ± 15	12	0.847	12 ± 2	0.1	26	0.827
GO-Lys	172 ± 20	102	0.952	73 ± 14	0.1	34	0.864

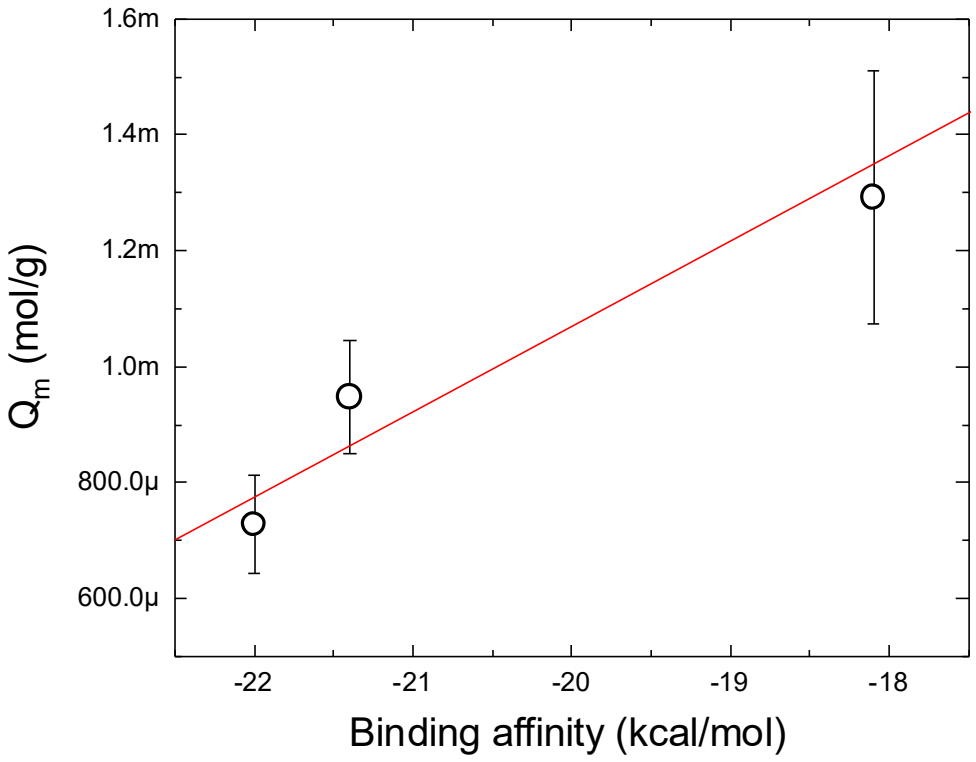

Fig. S10. Correlation plot between Qm measured by Adsorption kinetic experiments and the calculated Binding affinity.

Bibliography

1. J. Xu, L. Wang and Y. Zhu, *Langmuir*, 2012, **28**, 8418-8425.
2. M. H. Dehghani, M. Ghadermazi, A. Bhatnagar, P. Sadighara, G. Jahed-Khaniki, B. Heibati and G. McKay, *Journal of Environmental Chemical Engineering*, 2016, **4**, 2647-2655.
3. W. Libbrecht, K. Vandaele, K. De Buysser, A. Verberckmoes, J. W. Thybaut, H. Poelman, J. De Clercq and P. Van Der Voort, *Materials*, 2015, **8**, 1652-1665.
4. M. H. Dehghani, A. H. Mahvi, N. Rastkari, R. Saeedi, S. Nazmara and E. Iravani, *Desalination and Water Treatment*, 2015, **54**, 84-92.
5. H. Kono, K. Onishi and T. Nakamura, *Carbohydrate Polymers*, 2013, **98**, 784-792.
6. Q. Zhou, Y. Wang, J. Xiao and H. Fan, *Synthetic Metals*, 2016, **212**, 113-122.
7. A. Nezhadali, S. E. Koushali and F. Divsar, *Journal of Environmental Chemical Engineering*, 2021, **9**, 105648.
8. D. A. Borisova, M. D. Vedenyapina, E. D. Strel'tsova, V. L. Maslov, K. H. Rosenwinkel, D. Weichgrebe, P. Stopp and A. A. Vedenyapin, *Solid Fuel Chemistry*, 2013, **47**, 298-302.
9. H. M. Abdel-Aziz, R. S. Farag and S. A. Abdel-Gawad, *International Journal of Environmental Research*, 2019, **13**, 843-852.
10. S. U. Yoon, B. Mahanty and C. G. Kim, *Desalination and Water Treatment*, 2016, **57**, 7789-7800.
11. G. Liang, Z. Hu, Z. Wang, X. Yang, X. Xie and J. Zhao, *Environmental Science and Pollution Research*, 2020, **27**, 45435-45446.
12. X. Zhou, Y. Yang, C. Li, Z. Yang, W. Yang, Z. Tian, L. Zhang and T. Tao, *Journal of Cleaner Production*, 2018, **203**, 655-663.